IJMS

Original Article

Differential Effects of Single and Combined Anabolic–Androgenic Steroids on Male Fertility and Early Embryo Development in Exercised Mice

Leila Najafi[1], PhD candidate; Soghra Bahmanpour[1,2,3], PhD; Tahereh Esmaeilpour[1], PhD; Narges Karbalaei[4,5], PhD; Farzaneh Dehghani[1,5], PhD

[1]Department of Anatomical Sciences, School of Medicine, Shiraz University of Medical Sciences, Shiraz, Iran;
[2]Department of Reproductive Biology, School of Advanced Medical Sciences and Technologies, Shiraz University of Medical Sciences, Shiraz, Iran;
[3]Infertility Research Center, Shiraz University of Medical Sciences, Shiraz, Iran;
[4]Department of Physiology, School of Medicine, Shiraz University of Medical Sciences, Shiraz, Iran;
[5]Histomorphometry and Stereology Research Center, Shiraz University of Medical Sciences, Shiraz, Iran

Correspondence:
Farzaneh Dehghani, PhD;
Department of Anatomical Sciences, School of Medicine, Shiraz University of Medical Sciences, Zand Blvd.,
Postal code: 71348-45794, Shiraz, Iran
Tel: +98 71 32304372
Email: dehghanf@sums.ac.ir
Received: 22 January 2026
Revised: 20 May 2026
Accepted: 06 July 2026

What's Known

- Non-medical use of anabolic–androgenic steroids (AAS) disrupts spermatogenesis, reproductive hormones, sperm quality, and redox balance, often leading to testicular atrophy.
- Intense physical exercise may exacerbate AAS-induced reproductive dysfunction, yet downstream fertilization and embryonic outcomes remain poorly characterized.

What's New

- This study directly compares single versus combined AAS exposure under exercise conditions, revealing synergistic reproductive toxicity with combined regimens.
- Structural and sperm impairments translated into reduced fertilization, impaired cleavage, and poor embryo quality after *in vitro* fertilization (IVF), while serum testosterone levels alone were insufficient to predict functional reproductive competence.

Abstract

Background: The non-medical use of anabolic–androgenic steroids (AAS), particularly in multi-drug regimens, has become prevalent among athletes and may impair male fertility. However, their comparative effects on functional male fertility and early embryonic development remain poorly defined. This study aimed to compare the impacts of single and combined AAS on male reproductive health and early embryo development in a murine model of intense exercise.

Methods: Forty-two adult Swiss male mice were allocated to six groups for 4 weeks: Control, Sham (exercise only), Trenbolone+Exercise (150 mg/Kg/week), Testosterone+Exercise (300 mg/Kg/week), Nandrolone+Exercise (100 mg/Kg/week), and Combined group (all three AAS). Testicular and prostate architectures were assessed using unbiased stereology. Sperm quality, chromatin density, serum testosterone, and malondialdehyde concentration were measured. Functional fertility was evaluated through *in vitro* fertilization and embryo development. Data were analyzed using one-way ANOVA with Tukey's *post hoc* test ($P<0.05$).

Results: Testosterone, Nandrolone, and particularly combined AAS reduced testicular volume, seminiferous tubule length, and germ, Sertoli, and Leydig cell numbers. These alterations were accompanied by impaired sperm parameters, increased oxidative stress, and elevated prostate estimations (volume, luminal surface, and vascular length). Serum testosterone showed variable changes. Fertilization rate dropped from 95.4±8.6 (control) to 37.7±27.5 (combined group) ($P<0.001$). Cleavage ($P<0.01$) and embryo quality ($P<0.001$) were compromised, with the strongest impairments following combined AAS administration.

Conclusion: AAS "stacking" under exercise induces excessive structural and functional reproductive toxicity, which cannot be inferred from hormonal measurements alone. When sperm quality falls below a certain threshold, fertilization and early embryo development are impaired, especially following a multi-drug AAS regimen.

Please cite this article as: Najafi L, Bahmanpour S, Esmaeilpour T, Karbalaei N, Dehghani F.Differential Effects of Single and Combined Anabolic–Androgenic Steroids on Male Fertility and Early Embryo Development in Exercised Mice. Iran J Med Sci. doi: 10.30476/ijms.2026.110526.4623.

Keywords ● Anabolic aents ● Oxidative stress ● Embryo development ● Histology

Copyright: ©Iranian Journal of Medical Sciences. This is an open-access article distributed under the terms of the Creative Commons Attribution-NoDerivatives 4.0 International License. This license allows reusers to copy and distribute the material in any medium or format in unadapted form only, and only so long as attribution is given to the creator. The license allows for commercial use.

Introduction

Infertility remains a major global health challenge, with male factors contributing to nearly half of affected couples. Key determinants of male infertility, including reduced sperm concentration, impaired motility, and abnormal morphology, are frequently attributed to disruptions in the hypothalamic-pituitary-testicular (HPT) axis, defects in spermatogenesis, and deficiencies in the ductal system. These abnormalities may be influenced by environmental exposures, lifestyle factors, and strenuous physical activity.[1] Despite the health benefits of regular and moderate exercise (VO_{2max}<70%), research shows that intense or prolonged exercise (VO_{2max}>70%) without adequate recovery can act as a physiological stressor that reduces endogenous testosterone production, disrupts spermatogenesis, and negatively affects semen quality.[2]

Concurrently, the use of anabolic–androgenic steroids (AAS) has risen sharply among both competitive and recreational athletes.[3] These synthetic testosterone derivatives, commonly including testosterone, nandrolone, boldenone, and trenbolone, are often consumed at supraphysiological doses or in multi-drug "stacking" regimens to enhance anabolic outcomes.[3, 4] Despite their widespread misuse, AAS are associated with multisystem toxicities, among which male reproductive dysfunction represents one of the most consistently reported and clinically relevant consequences.[5]

Notably, the reproductive effects of AAS exposure remain controversial. While some studies have reported partial preservation or recovery of spermatogenesis following AAS administration,[6, 7] a larger body of evidence demonstrates hormonal disorders, testicular atrophy, abnormal spermatogenic arrest, reduced libido, erectile dysfunction, and adverse prostate alterations.[5, 8]

Both strenuous exercise and AAS exposure can also promote excessive reactive oxygen species (ROS) generation.[9, 10] Because testicular tissue and spermatozoa contain high levels of polyunsaturated fatty acids and have relatively weak antioxidant defenses, they are particularly susceptible to oxidative damage. The ROS overproduction can induce lipid peroxidation, mitochondrial dysfunction, and chromatin abnormalities, ultimately impairing sperm parameters and fertilization potential.[11, 12]

The quantity and quality of spermatozoa are critical determinants of fertilization success and early embryonic development. Beyond delivering paternal DNA, sperm contribute essential epigenetic regulators, including small RNAs and DNA methylation patterns, which become particularly important during zygotic genome activation at the 2- to 8-cell stage.[13] Evidence indicates that sperm DNA damage can disrupt cleavage dynamics, impair embryo morphology, and reduce blastocyst formation, highlighting the limitations of conventional semen analysis alone.[14]

Despite growing concerns regarding AAS misuse, several critical gaps remain. In particular, the comparative reproductive toxicity of individual versus combined AAS regimens under conditions of intense physical activity is poorly defined. Notably, while AAS-induced testicular alterations have been widely reported,[5, 11] few data are known about how these alterations translate into functional defects during the earliest stages of embryogenesis.[15] In this context, *in vitro* fertilization (IVF)-based embryo assessment provides a sensitive and integrative measure of sperm functional competence.

Therefore, this study aimed to investigate the structural and functional reproductive consequences of three commonly misused AAS, namely testosterone, nandrolone, and trenbolone, administered alone or in combination in exercised male mice. Specifically, we sought to determine whether multi-drug AAS stacking produces more severe reproductive toxicity than individual compounds, and whether standard sperm parameter alterations translate into impaired early embryo development.

Materials and Methods

Chemicals

Testosterone Enanthate (Test) (100 mg/mL, Iran Hormone, Iran), Nandrolone Decanoate (ND) (25 mg/mL, Iran Hormone, Iran) and Trenbolone Enanthate (TR) (200 mg/mL, Iron Pharma, Malaysia) were purchased. These drugs were in injectable vials and in liquid form. Unopened vials were kept at room temperature (22-25 °C). After opening, the solutions were stored at 4 °C in a refrigerator.

Animals

Forty-two adult male Swiss mice (7–8 weeks old; 28–30 g) were recruited for the experiment. Animals were kept under standardized laboratory conditions (22±2 °C; 12 h light/dark cycle) at the animal facility of Shiraz University of Medical Sciences, with unrestricted access to water and a standard pellet diet.

Experimental Design

After a 7-day adaptation period, the mice were allocated into six groups (n=7 per group).

Animals were randomly allocated to groups by an investigator not involved in the study and blinded to the experimental protocol. Each cage was then assigned to one of the following groups:

- Control: No treatment or exercise
- Sham: Exercise only (3 sessions/week, 4 weeks)
- TR+Ex: TR (150 mg/Kg/week; intraperitoneal)+Exercise
- Test+Ex: Test (300 mg/Kg/week; intraperitoneal)+Exercise
- ND+Ex: ND (100 mg/Kg/week; intraperitoneal)+Exercise
- Combined AAS+Ex: [TR+Test+ND] at the above doses+Exercise

The initial doses were selected based on: (1) the commercial multi-steroid preparation Pharma MIX 3 (Test: ND: TR=200:200:100 mg/mL; 2:2:1 ratio), (2) studies that have administered ND at 300 mg/Kg/week,[16, 17] and (3) a pilot dose optimization. The starting doses were therefore set as Test 300, ND 300, and TR 150 mg/Kg/week.

During piloting, ND 300 mg/Kg/week caused unacceptable mortality, likely due to synergistic toxicity. ND was stepwise reduced to 200 and then 100 mg/Kg/week.[17] At 100 mg/Kg/week, no mortality occurred. The Test and TR doses remained unchanged due to technical constraints (minimum draw volume for TR) and pharmacological evidence that TR is 3-5 times more potent than Test.[18]

Based on allometric scaling (mouse-to-human conversion factor of 12.3),[19] these doses approximate the upper range of human AAS abuse patterns (10–100 times the therapeutic levels).[4]

Intraperitoneal delivery was selected due to its high vascularity and reliable systemic absorption.[20] The 4-week exposure was chosen to span the complete duration of murine spermatogenesis.[21]

One week after the last injection, animals were sacrificed using CO_2 inhalation. Reproductive tissues (epididymis with attached vas deferens, prostate, left seminal vesicle, and left testis) were harvested through a midline abdominal incision. The right epididymis and vas deferens were processed for sperm evaluation, and the left side was used for oxidative stress assessment. All remaining tissues were fixed for stereological analysis.

Exercise Protocol

Mice underwent swimming exercise in a plastic tank (43×34×26 cm) for 15 min/session with sufficient depth to avoid tail or limb contact with the bottom surface. Water temperature was maintained at 24–26 °C to minimize stress.[22]

Body and Organ Weights

Body weight was recorded at the start of the experiment (W1) and before euthanasia (W2). The gain in body weight was calculated as:[23]

Body weight gain (%)=(W2-W1)/W1×100

Left testis, left seminal vesicle, and prostate were weighed immediately after dissection.

Serum Testosterone Measurement

Under deep anesthesia, blood samples (≈2 mL) were collected via cardiac puncture. Serum was separated after centrifugation (3000 rpm, 10 min) and stored at -20°C until analysis. Testosterone concentrations were measured using a commercial enzyme-linked immunosorbent assay (ELISA) kit (Monobind, USA) according to the manufacturer's instructions, and results were expressed in ng/mL.[24]

Sperm Preparation

The epididymis with vas deferens was placed in 1 mL pre-warmed Ham's F10 medium (Fertilite, Iran), and gently minced to allow sperm to swim out. The sample was then incubated (37 °C, 5 % CO2) for 10 min to support sperm capacitation.[25, 26]

Sperm Count, Motility, Viability, and Morphology

Sperm concentration was determined using a Neubauer chamber. At least 200 spermatozoa were examined per sample for motility (progressive, non-progressive, immotile) and viability (eosin staining). Morphology was evaluated on Papanicolaou-stained slides following World Health Organization (WHO) criteria.[25]

Chromomycin A3 (CMA3) Assay

Protamine deficiency was assessed using CMA3 (Sigma, USA) staining. Air-dried smears were fixed in Carnoy's solution (methanol:acetic acid, 3:1) for 10 min at 4 °C, then stained with CMA3 solution (0.25 mg/mL in McIlvain buffer) for 20 min in darkness. At least 200 spermatozoa were examined under a fluorescence microscope (Olympus, Japan; 460–470 nm). Bright yellow fluorescence in spermatozoa indicated CMA3 positivity.[27]

Oxidative Stress Assessment

The amount of ROS produced in the sperm sample was assessed by measuring malondialdehyde (MDA) levels as an indicator of lipid peroxidation using the thiobarbituric acid reactive substances (TBARS) method. Thus, sperm samples were homogenized by

sonication on ice. Total protein concentration was measured using a bicinchoninic acid (BCA) assay (Parstous, Iran). For MDA analysis, 200 µL of sample was mixed with trichloroacetic acid (TCA) (20%) (Sigma, USA) and thiobarbituric acid (TBA) (0.8%) (Sigma, USA) and incubated at 87 °C for 1 hour. After cooling and centrifugation (4000 rpm, 10 min), absorbance was measured at 532 nm using a microplate reader (Biotek, Synergy HT, USA). Data were expressed as nmol/mg protein.[28]

Stereological Analysis

Primary volumes (Vprimary) of the testis, prostate, and seminal vesicle were estimated by the immersion technique. After fixation, isotropic uniform random (IUR) sections of the testis and prostate were prepared using the orientator method. Hematoxylin and eosin (H&E) staining was performed with Harris hematoxylin (Bio Optica, Italy) and Eosin Y (1% aqueous solution, Bio Optica, Italy). All histological slides were examined under a light microscope (Olympus CX41, Japan). Tissue shrinkage during processing was also considered for the testis.[29]

Volume Shrinkage and Testicular Total Volume Estimation

Shrinkage was quantified by comparing pre- and post-processing areas of circular punches:[29]
Volume shrinkage=1-(AA/AB)$^{1.5}$
AA and AB: post- and pre-processing areas
$V_{final}=V_{primary}\times$(1-Volume shrinkage)

Volume of Testicular Structures

Volume densities of seminiferous tubules and interstitial tissue were estimated using point-counting of 5 µm sections at 390× magnification:[29]

$$Vv_{\left(\frac{structure}{testis}\right)}=\frac{\sum p_{structure}}{\sum p_{Total}}$$

"$\sum P_{Structure}$": the point numbers hitting the tubules or interstitial tissue
"$\sum P_{Total}$": the point numbers hitting the testis
Total volume:
$V_{(structure)}=Vv_{(structure/testis)}\times V_{final}$ (mm^3)

Germinal Epithelium and Leydig Cell Counts

Cell numbers were estimated in 25-µm sections using the optical disector method with a 15-µm disector height and a 40×oil-immersion objective lens (total magnification:1500×). Numerical density was calculated as:[29]

$$N_V=\frac{\sum Q}{\sum p\times(a/f)\times h}\times\frac{t}{BA}$$

"∑Q": the number of cells counted within the disector height, "∑P": the total number of observed frames, "a/f": the area of the counting frame, "h": the height of the disector (15 µm), "BA": the microtome setting, "t": the mean final section thickness.
Total number of cells:
$N=N_v\times V_{final}$

Length of Seminiferous Tubules and Prostatic Vessels

Length density was calculated in 5µm tissue sections using a counting frame at 150× (tubules) and 390× (vessels) magnifications:[30]

$$L_V=\frac{2\times\sum Q}{(a/f)\times\sum p}$$

"∑Q": the total count of tubular or vascular profiles, "a/f": the area of the applied counting frame, "∑p": the total number of frames.
Total length:
$L=L_v\times V_{final}$

Luminal Surface of the Prostate

The luminal surface was estimated using 5 µm sections and a counting frame at 390× magnification:[30]

$$\text{Total surface}=\frac{2\times\sum I}{l/p\times\sum P}\times V_{prostate}$$

"∑I": the total number of times the test lines intersect with the luminal surface, "l/p": the test line length corresponding to each point on the grid, "∑P": the total number of points located within the defined reference area.

IVF and Embryo Assessment

Oocyte Collection: Female mice (8–10 weeks) were superovulated with 10 IU pregnant mare's serum gonadotrophin (PMSG) (Radin Dam, Iran) followed 48 h later by 10 IU human chorionic gonadotrophin (hCG) (Rooyan Darou, Iran). After 13–15 hours, cumulus–oocyte complexes (COCs) were retrieved from the ampullary region of the oviduct.[26]

Fertilization Procedure and Embryo Culture: COCs were transferred into pre-equilibrated fertilization drops (single+ culture medium, Fertilite, Iran) (50 µL) under mineral oil (RS Medical, Iran). An identical volume of capacitated sperm suspension (50 µL) was added, and fertilization was allowed for 4–6 hours. Zygotes were then washed and moved to fresh culture drops.

Embryos were cultured at 37 °C in 5% CO_2, with daily transfer into new drops. Development was monitored at 24, 48, and 72 hours

post-insemination using a stereomicroscope (Optika SZM-3, Italy).[26]

Fertilization and Cleavage Rates: The fertilization rate was calculated based on the presence of two pronuclei (2PN) relative to the total number of retrieved COCs. Embryo cleavage was evaluated on Day 3 after insemination, and the cleavage rate was defined as the proportion of cleaved embryos relative to the number of fertilized oocytes. Embryos were classified according to their developmental stage (2-cell, 4-cell, 6-cell and 8-cell), and the percentage distribution across these stages was documented.[26]

Embryo Morphology and Quality Scoring: Embryos were graded based on blastomere symmetry, fragmentation, and cytoplasmic appearance (A–D). A composite Day-3 quality score was calculated by combining developmental stage (2–8 cells=1–4 points) and morphology grade (A–D=4–1 points), yielding a maximum score of 8.[31, 32]

A. Equal-sized blastomeres without cytoplasmic fragments

B. A minor inequality in blastomere size with up to 20% cytoplasmic fragments

C. Unequal-sized blastomeres with 20-50% cytoplasmic fragments

D. Unequal-sized blastomeres with abundant cytoplasmic fragments and >50% dark granules

Ethical Consideration

All procedures were conducted according to institutional ethical standards and approved by the Ethics Committee of Shiraz University of Medical Sciences, Iran (IR.SUMS.AEC.1401.095).

Statistical Analysis

Data are presented as mean±SD. Normality was assessed using the Shapiro-Wilk test. Normally distributed data were analyzed using one-way ANOVA with Tukey's *post hoc* test, while non-normally distributed or non-homogeneous data (cleavage rates) were analyzed using Kruskal-Wallis with Dunn's *post hoc* test. Analyses were performed using GraphPad Prism 8.4.3 (GraphPad Software, USA), and a P value <0.05 was considered statistically significant.

Table 1: Mean±SD of body weight, organ weight, and organ volume among different experimental groups

Variable		Control	Sham	TR +Es	Test +Es	P value	ND+Es	P value	Combined AAS+Es	P value
Body weight gain (%)		12.05± 1.13	10.03± 1.58	9.67± 1.34	8.32± 2.63[a]	a: P=0.001	6.35± 1.31[abc]	a: P<0.001; b: P=0.001; c: P=0.005	4.91± 0.93[abcd]	a: P<0.001; b: P<0.001; c: P<0.001; d: P=0.003
Organ weight (g)	Testis	0.13± 0.004	0.12± 0.011	0.10± 0.007	0.09± 0.018[a]	a: P=0.01	0.08± 0.004[ab]	a: P<0.001; b: P=0.01	0.06± 0.004[abcd]	a: P<0.001; b: P<0.001; c: P<0.001; d: P=0.003
	Prostate	0.11± 0.004	0.13± 0.015	0.14± 0.019	0.16± 0.030[a]	a: P=0.007	0.17± 0.036[a]	a: P=0.003	0.19± 0.037[abc]	a: P<0.001; b: P=0.01; c: P=0.04
	Seminal vesicle	0.15± 0.025	0.16± 0.026	0.21± 0.043	0.34± 0.095[ab]	a: P=0.01 b: P=0.01	0.40± 0.068[abc]	a: P<0.001; b: P<0.001; c: P=0.003	0.45± 0.128[abc]	a: P<0.001; b: P<0.001; c: P<0.001
Organ volume (cm3)	Testis	0.11± 0.004	0.10± 0.011	0.10± 0.004	0.07± 0.018[a]	a: P=0.01	0.06± 0.004[abc]	a: P<0.001; b: P=0.01; c: P=0.02	0.04± 0.004[abcde]	a: P<0.001; b: P<0.001 c: P<0.001; d: P=0.002; e: P=0.04
	Prostate	0.09± 0.004	0.11± 0.015	0.12± 0.019	0.14± 0.030[a]	a: P=0.007	0.15± 0.036[a]	a: P=0.003	0.17± 0.037[abc]	a: P<0.001; b: P=0.01; c: P=0.04
	Seminal vesicle	0.13± 0.025	0.14± 0.026	0.19± 0.043	0.32± 0.095[ab]	a: P=0.01; b: P=0.01	0.38± 0.068[abc]	a: P<0.001; b: P<0.001; c: P=0.003	0.43± 0.128[abc]	a: P<0.001; b: P<0.001; c: P<0.001

Data were analyzed using one-way ANOVA followed by Tukey's *post hoc* test. Different letters (a, b, c, d, and e) indicate significant differences with Control, Sham, TR, Test, and ND groups. TR: Trenbolone enanthate; Test: Testosterone enanthate; ND: Nandrolone decanoate; Combined AAS: TR+Test+ND

Results

Body Weight and Organ Weights and Volumes

All AAS-treated groups showed reduced body weight gain compared with the control group, reaching significance in Test (P=0.001), ND, and Combined AAS (both P<0.001), whereas the Sham and TR groups exhibited minimal, non-significant changes (table 1).

In parallel, testicular weight and volume were significantly reduced in the Test (P=0.01), ND, and especially the Combined groups (both P<0.001), although the pattern of significant differences among groups was slightly broader for testicular volume (table 1).

In contrast, both prostate and seminal vesicle weights and volumes increased markedly in all intervention groups. Prostate volume and weight were significantly elevated in the Test (P=0.007), ND (P=0.003), and Combined AAS groups (P<0.001), with the Combined group showing higher values than both sham (P=0.01) and TR (P=0.04) groups.

Similarly, seminal vesicle volume and weight rose significantly in the Test (P=0.01), ND, and Combined groups (both P<0.001) compared with control and sham, and were further elevated in the ND (P=0.003) and Combined (P<0.001) groups relative to TR (table 1).

Sperm Parameters and Chromatin Condensation

Sperm count markedly declined in the Test ($25.71\pm5.31\times10^6$), ND ($17\pm4.24\times10^6$), and Combined groups ($15.71\pm1.38\times10^6$) compared with control ($40.14\pm6.74\times10^6$) (P<0.001). The Combined AAS group displayed significantly lower sperm counts compared to the sham, TR (both P<0.001), and Test (P=0.005) groups (figure 1).

Across all intervention groups, sperm motility, viability, and morphology were significantly compromised, with the most notable impairments observed in the Test, ND, and Combined groups (all P<0.001). Chromatin condensation defects, assessed by CMA3 staining, also increased significantly in all AAS-treated (P<0.001) and Sham groups (P=0.003), with the Combined group showing the highest proportion of CMA3-positive spermatozoa (P<0.001). Intergroup comparisons are shown in figure 1.

Testosterone Levels

Serum testosterone levels remained comparable to controls in the Sham, TR, and ND groups.

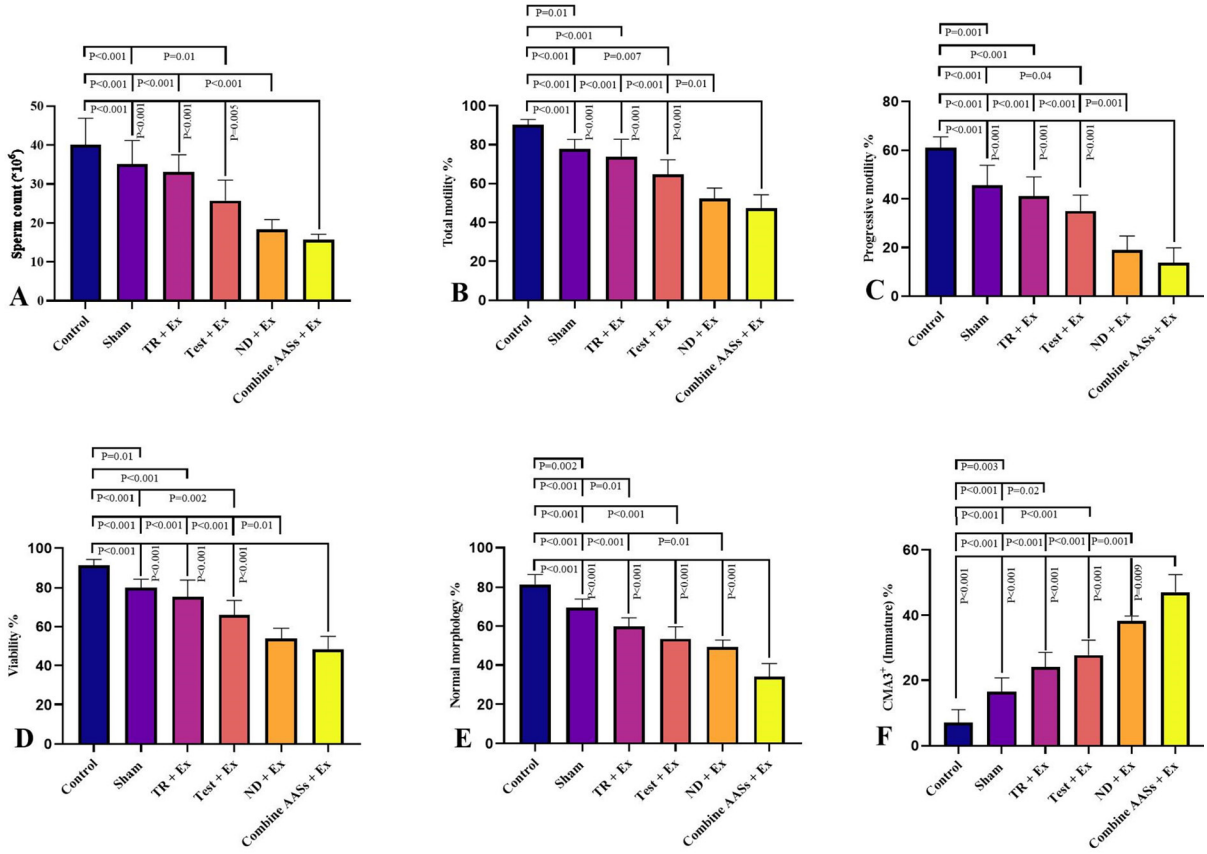


Figure 1: This figure presents the mean±SD of sperm parameters and chromatin packaging in different experimental groups. The graphs show data for (A) sperm count, (B) total motility, (C) progressive motility, (D) viability, (E) normal morphology, and (F) immature chromatin. Data were analyzed using one-way ANOVA followed by Tukey's *post hoc* test. TR: Trenbolone enanthate; Test: Testosterone enanthate; ND: Nandrolone decanoate; Combined AAS: TR+Test+ND

In contrast, both Test and Combined AAS groups showed a marked elevation in testosterone concentrations (P<0.001 vs. Control, Sham, TR, and ND). Testosterone levels did not differ significantly between Test and Combined AAS groups (figure 2A).

MDA Levels

Lipid peroxidation was significantly elevated in Test (0.96±0.25 nmol/mg protein) (P=0.02), ND (0.98±0.20 nmol/mg protein) (P=0.01), and Combined groups (1.23±0.35 nmol/mg protein) (P<0.001) compared to control (0.51±0.14 nmol/mg protein). The Combined regimen also differed significantly from sham and TR (both P<0.01), while no other intergroup differences were significant (figure 2B).

Histological and Stereological Study

Testis

Histopathological examination revealed progressive testicular alterations in the AAS-treated groups, characterized by germinal epithelium and Leydig cell degeneration, reduced spermatogenic cell density, disruption of seminiferous tubule architecture, lumen expansion, interstitial edema, and increased acidophilic stromal areas. The severity of changes increased from Test to ND and was most pronounced in the Combined AAS group. In contrast, the Sham and TR groups exhibited only mild changes in some sections (figure 3).

Seminiferous Tubule and Interstitial Tissue Volumes

As shown in table 2, seminiferous tubule volume was reduced in all intervention groups, most markedly under the Combined regimen, which differed significantly from every other group (with Control, Sham, TR, and Test: P<0.001; with ND: P=0.003). Test (P=0.002 and P=0.01, respectively) and ND (P<0.001) groups also differed significantly from sham and TR groups.

Interstitial tissue volume showed the opposite pattern, with significant expansion in Test, ND, and Combined AAS groups (P<0.001). In addition, the Combined administration showed greater expansion than both Sham (P=0.01) and TR (P=0.03) groups, and the ND group also differed significantly from the sham group (P=0.03) (table 2).

Total Length of Seminiferous Tubules

Tubule length decreased in the Sham and all AAS-treated groups, reaching significance in the Test, ND, and especially the Combined groups (P<0.001). The Combined AAS also differed significantly from Sham, TR (both P<0.001), and Test (P=0.001) groups. ND presented similar reductions versus Sham (P=0.001) and TR (P=0.008) (table 2).

Germinal Epithelium and Leydig Cell Numbers

Test (spermatocyte: P=0.002; spermatid, sperm, Sertoli, and Leydig: P=0.01), ND (spermatocyte, spermatid, and Sertoli: P<0.001; sperm: P=0.002; Leydig: P=0.009) and especially Combined AAS (all P<0.001) exposures reduced the numbers of all germ cell lineages, Sertoli, and Leydig cells.

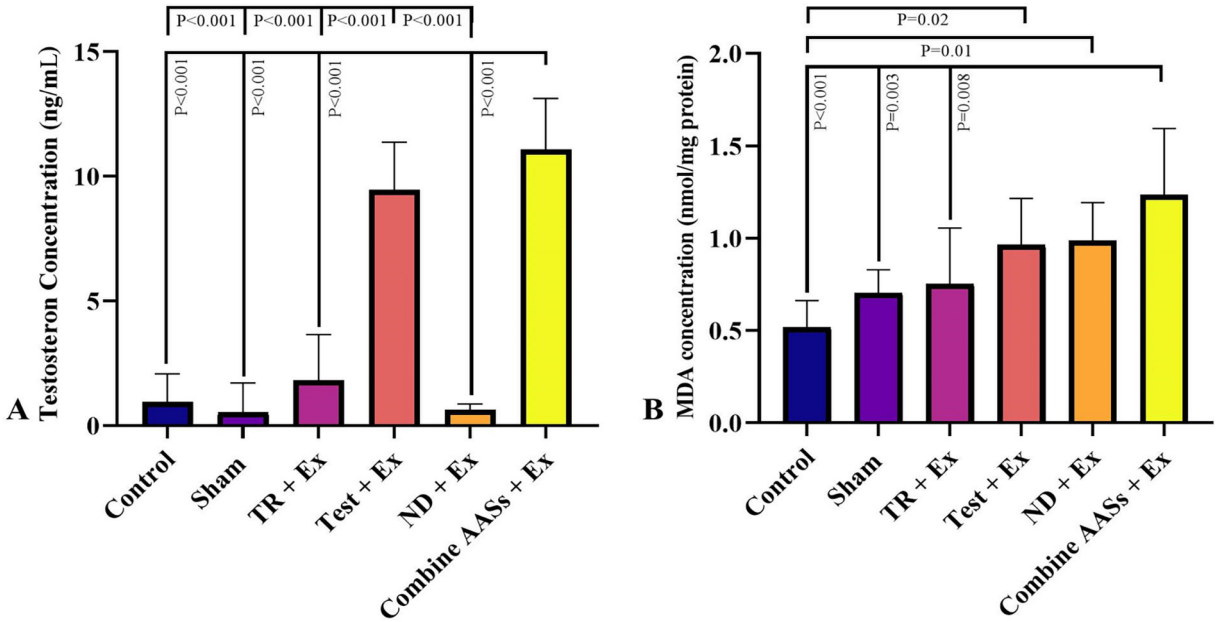


Figure 2: This figure shows the mean±SD of serum testosterone (A) and sperm sample malondialdehyde (MDA) (B) levels in different experimental groups. Data were analyzed using one-way ANOVA followed by Tukey's *post hoc* test. TR: Trenbolone enanthate; Test: Testosterone enanthate; ND: Nandrolone decanoate; Combined AAS: TR+Test+ND

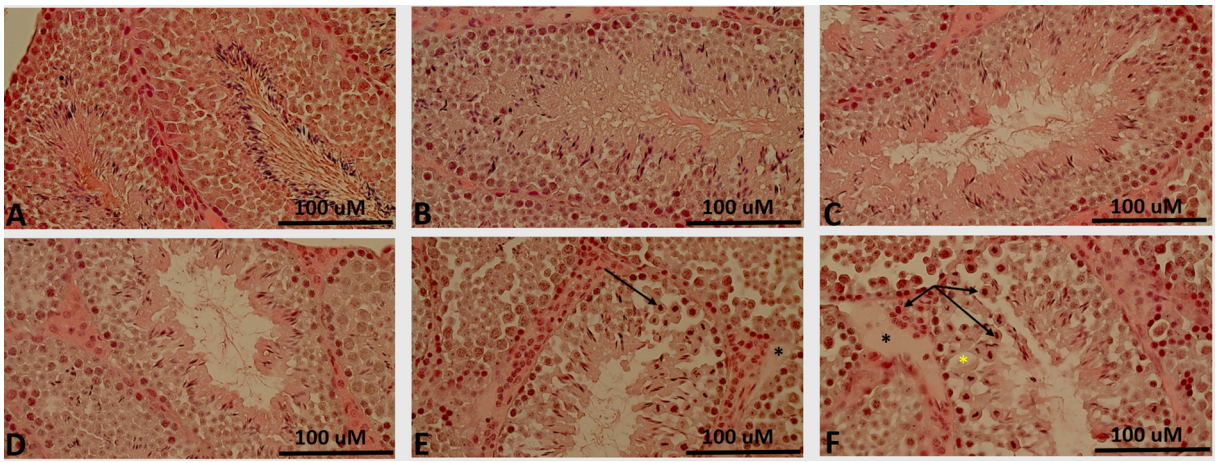


Figure 3: Photomicrographs of H&E-stained testicular sections in different experimental groups are shown. The control group (A) shows normal spermatogenesis, while the Sham (B), TR (C), Test (D), ND (E), and Combined AAS (F) groups exhibit reduced spermatogenic cells, increased interstitial tissue, and lumen dilation. Severe Leydig and germ cell degeneration (indicated by arrows), vacuolated cytoplasm (yellow asterisk), and acidophilic material (black asterisks) are particularly observed in the ND and Combined groups. Scale bar: 100 µm. TR: Trenbolone enanthate; Test: Testosterone enanthate; ND: Nandrolone decanoate; Combined AAS: TR+Test+ND

Table 2: Mean±SD of seminiferous tubule and interstitial space volume and the length of the seminiferous tubule among different experimental groups

Variable	Control	Sham	TR+Ex	Test+Ex	P value	ND+Ex	P values	Combined AAS+Ex	P value
Seminiferous tubules volume (mm^3)	94.57± 4.75	83.06± 8.82	80.33± 4.88	62.44± 13.87^{abc}	a: P<0.001; b: P=0.002; c: P=0.01	54.38± 3.70^{abc}	a: P<0.001 b: P<0.001 c: P<0.001	34.27± 3.67^{abcde}	a: P<0.001; b: P<0.001; c: P<0.001; d: P<0.001; e: P=0.003
Interstitial space volume (mm^3)	8.24± 0.90	12.00± 2.26	12.79± 1.77	17.10± 4.79^{a}	a: P<0.001	17.40± 2.23^{ab}	a: P<0.001; b: P=0.03	18.11± 1.98^{abc}	a: P<0.001; b: P=0.01; c: P=0.03
Seminiferous tubule length (mm)	2804± 483.8	1986± 276.4	1849± 318.9	1528± 325.9^{a}	a: P<0.001	1170± 242^{abc}	a: P<0.001; b: P=0.001; c: P=0.008	732.6± 99.35^{abcd}	a: P<0.001; b: P<0.001; c: P<0.001; d: P=0.001;

Data were analyzed using one-way ANOVA followed by Tukey's *post hoc* test. Different letters (a, b, c, d, and e) indicate significant differences among the Control, Sham, TR, Test, and ND groups. TR: Trenbolone enanthate; Test: Testosterone enanthate; ND: Nandrolone decanoate; Combined AAS: TR+Test+ND

Table 3: Mean±SD of the number of spermatogonia, spermatocytes, spermatids, sperm, Sertoli, and Leydig cells ($\times 10^6$) among different experimental groups

Variable	Control	Sham	TR+Ex	Test+Ex	P values	ND+Ex	P values	Combined AAS+Ex	P values
Spermatogonia	12.64± 6.14	10.51± 3.72	8.53± 1.55	7.76± 3.52		4.23± 0.91^{ab}	a: P=0.007; b: P=0.04	3.75± 0.62^{ab}	a: P=0.004; b: P=0.02
Spermatocyte	16.91± 3.60	13.59± 2.28	12.04± 1.59	9.54± 4.26^{a}	a: P=.002	6.15± 0.64^{abc}	a: P<0.001; b: P=0.001; c: P=0.01	4.98± 0.36^{abc}	a: P<0.001; b: P<0.001; c: P=0.002
Spermatid	47.61± 13.26	40.73± 8.50	35.32± 13.88	24.55± 10.08^{a}	a: P=0.01	15.85± 4.71^{abc}	a: P<0.001; b: P=0.004; c: P=0.03	6.46± 1.80^{abc}	a: P<0.001; b: P<0.001; c: P=0.001
Sperm	59.70± 25.92	47.72± 9.44	44.65± 13.06	28.99± 12.24^{a}	a: P=0.01	21.12± 6.58^{ab}	a: P=0.002; b: P=0.03	8.97± 1.73^{abc}	a: P<0.001; b: P=0.001; c: P=0.002
Sertoli cell	3.24± 1.33	2.68± 0.14	2.49± 0.72	1.67± 0.42^{a}	a: P=0.01	1.23± 0.30^{abc}	a: P<0.001; b: P=0.01; c: P=0.03	1.01± 0.16^{abc}	a: P<0.001; b: P=0.003; c: P=0.01
Leydig cell	3.02± 0.44	2.37± 0.79	2.13± 0.13	1.85± 0.35^{a}	a: P=0.01	1.79± 0.54^{a}	a: P=0.009	1.13± 0.31^{abc}	a: P<0.001; b: P=0.005; c: P=0.03

Data were analyzed using one-way ANOVA followed by Tukey's *post hoc* test. Different letters (a, b, and c) indicate significant differences among the Control, Sham, and TR groups. TR: Trenbolone enanthate; Test: Testosterone enanthate; ND: Nandrolone decanoate; Combined AAS: TR+Test+ND

While, a significant reduction in spermatogonia cells count was observed in the ND (P=0.007) and triple AAS (P=0.004) groups. Sham and TR interventions exhibited mild declines that did not reach significance (table 3).

Prostate

Histopathological assessment of the prostate demonstrated distinct lobe-specific alterations. In the anterior lobe, marked glandular luminal dilation and increased intraluminal secretions were evident in the Test, ND, and Combined AAS groups, accompanied by pronounced epithelial thinning and reduced epithelial folding in the ND and particularly the Combined regimens. In the dorsolateral lobe, epithelial architectural disruption with epithelial cell hypertrophy and hyperplasia was observed, most prominently in the ND and Combined AAS groups (figures 4 and 5).

Prostate Luminal Surface and Vessel Length

The luminal surface of the prostate significantly expanded in the Test (P=0.007), ND (P=0.001) and most prominently in the Combined AAS group (P<0.001) relative to the control.

Blood vessel length within the prostate also increased significantly in Test (P=0.001), ND, and Combined AAS (both P<0.001) groups. The Combined group exhibited the most notable increase compared with the other groups. Furthermore, the ND showed higher values versus Sham and TR, and the Test group differed from Sham (table 4).

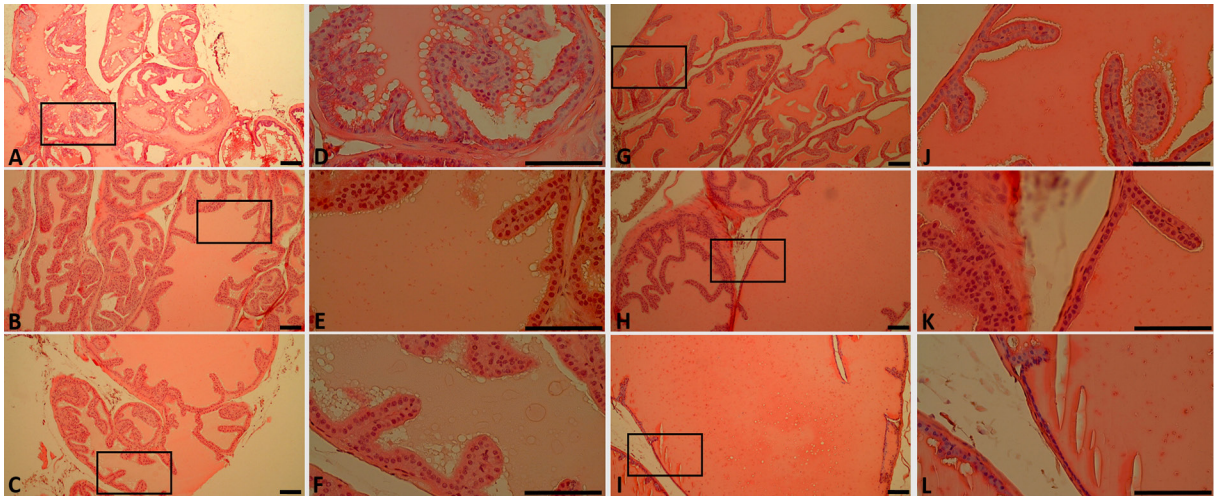


Figure 4: This figure represent photomicrographs of H&E-stained mouse anterior prostate sections at 100× and 400× magnifications in different experimental groups: Control (A, D), Sham (B, E), TR (C, F), Test (G, J), ND (H, K), and Combined AAS (I, L). The Test, ND, and especially the Combined AAS group display glandular lumen dilation, reduced epithelial thickness, increased intraluminal secretion, and decreased folding compared to the Control group. Scale bar: 100 µm. TR: Trenbolone enanthate; Test: Testosterone enanthate; ND: Nandrolone decanoate; Combined AAS: TR+Test+ND

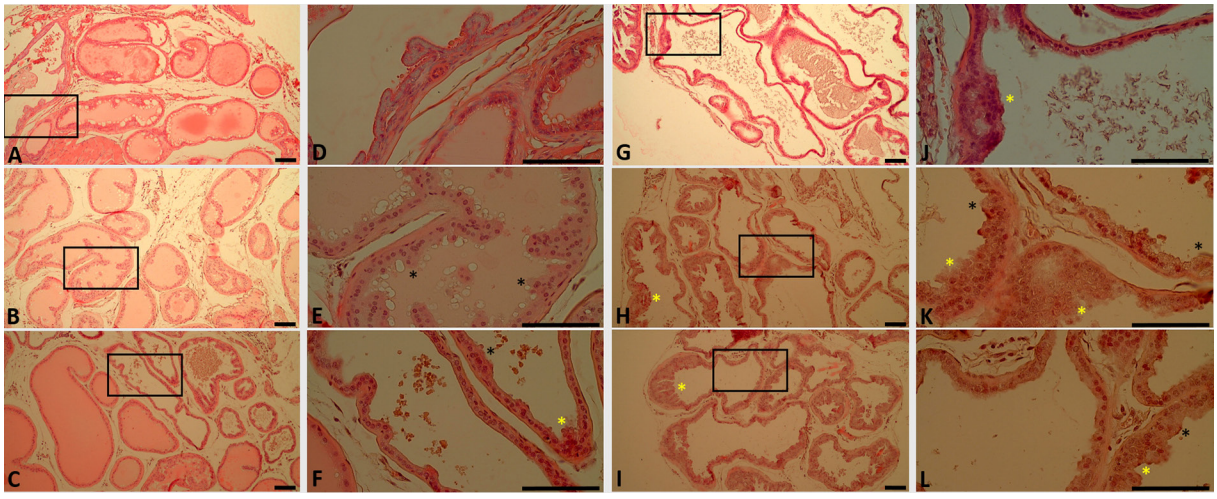


Figure 5: Photomicrographs of H&E-stained mouse dorsolateral prostate sections at 100× and 400× magnifications in different experimental groups: Control (A, D), Sham (B, E), TR (C, F), Test (G, J), ND (H, K), and Combined AAS (I, L). The Test, ND, and especially Combined AAS groups exhibit epithelial irregularity, hypertrophy (black asterisks), and hyperplasia (yellow asterisks). Scale bar: 100 µm. TR: Trenbolone enanthate; Test: Testosterone enanthate; ND: Nandrolone decanoate; Combined AAS: TR+Test+ND

Table 4: Mean±SD of the prostate luminal surface and vessel length among different experimental groups

Variable	Control	Sham	TR+Ex	Test+Ex	P value	ND+Ex	P values	Combined AAS+Ex	P value
Prostate luminal surface (mm^2)	652.8± 134	1207± 261	1295± 360.4	1563± 495.4[a]	a: P=0.007	1692± 244.8[a]	a: P=0.001	1866± 526.1[a]	a: P<0.001
Prostate vessel length (mm)	1893± 247.5	2762± 264.4	3159± 752.7	5295± 1399[ab]	a: P=0.001; b: P=0.02	5738± 929.6[abc]	a: P<0.001; b: P=0.005; c: P=0.01	9699± 2128[abcde]	a: P<0.001; b: P<0.001; c: P<0.001; d: P<0.001; e: P<0.001

Data were analyzed using one-way ANOVA followed by Tukey's *post hoc* test. Different letters (a, b, c, d, and e) indicate significant differences among the Control, Sham, TR, Test, and ND groups. TR: Trenbolone enanthate; Test: Testosterone enanthate; ND: Nandrolone decanoate; Combined AAS: TR+Test+ND

Table 5: Mean±SD of fertilization rate, total, 2-, 4-, 6-, and 8-cell cleavage rates, and quality score in embryos derived from adult male mice in different experimental groups

Varaible	Control	Sham	TR+Ex	P value	Test+ Ex	P value	ND+Ex	P values	Combined AAS+Ex	P value
Fertilization rate (%)	95.40± 8.61	89.59± 8.71	87.57± 11.75		73.11± 27.53		41.94± 12.80[abc]	a: P<0.001; b: P=0.001; c: P=0.002	37.71± 27.48[abcd]	a: P<0.001; b: P<0.001; c: P<0.001; d: P=0.01
Total cleavage rate (%)	98.21± 3.07	96.12± 4.92	95.92± 10.80		94.14± 12.45		94.29± 12.78		71.43± 48.80	
2-cell cleavage (%)	26.31± 14.27	37.11± 12.58	50.66± 22.23		54.54± 32.14		55.71± 44.15		52.38± 41.31	
4-cell cleavage (%)	25.85± 11.96	28.61± 9.16	20.49± 10.89		26.09± 26.35		28.57± 26.24		14.76± 20.35	
6-cell cleavage (%)	11.98± 5.64	10.10± 12.10	12.22± 11.21		11.31± 18.43		10± 22.36		4.28± 11.34	
8-cell cleavage (%)	34.04± 17.62	20.31± 20.73	12.56± 17.70		2.19± 5.81[a]	a: P=0.009	0[a]	a: P=0.005	0[a]	a: P=0.001
Embryo quality score	5.73± 0.57	4.62± 0.65	3.74± 0.51[a]	a: P<0.001	3.57± 0.59[a]	a: P<0.001	3.29± 0.89[a]	a: P<0.001	1.76± 1.23[abcde]	a: P<0.001; b: P<0.001; c: P<0.001; d: P=0.001; e: P=0.02

Data were analyzed using one-way ANOVA followed by Tukey's *post hoc* test (for fertilization rate and embryo quality) and Kruskal-Wallis followed by Dunn's *post hoc* test (for cleavage rates). Different letters (a, b, c, d, and e) indicate significant differences among the Control, Sham, TR, Test, and ND groups. TR: Trenbolone enanthate; Test: Testosterone enanthate; ND: Nandrolone decanoate; Combined AAS: TR+Test+ND

IVF and Embryo Assessment

Fertilization rates were highest in the Control (95.40±8.61 %) and Sham (89.59±8.71 %) groups, whereas ND (41.94±12.80 %) and particularly the Combined AAS group (37.71±27.48 %) showed marked reductions. ND and Combined AAS exhibited significantly lower fertilization compared with Control and Sham (P<0.001), with the Combined regimen also performing worse than TR (P<0.001) and Test (P=0.01) (table 5).

Cleavage progression on Day 3 displayed a similar pattern. While Control and Sham embryos reached advanced stages, TR showed only a mild delay. In contrast, Test, ND, and especially the Combined AAS group demonstrated substantial arrest at the 2–4-cell stages. The number of 8-cell embryos was reduced in the Test group, and no embryos reached this stage in the ND and Combined AAS groups. Only the 8-cell stage showed statistically significant reductions in these groups (P<0.01) (table 5).

Embryo quality scores declined progressively across the AAS-treated groups, with all steroid-treated animals showing significantly lower scores compared with controls (P<0.001). The Combined AAS group exhibited the most severe impairment, scoring significantly lower than all other intervention groups (P<0.05) (table 5).

Discussion

This study offers a comprehensive assessment of the structural, endocrine, and functional effects of individually administered versus combined regimens of three widely misused AAS under exercise-induced stress. Using simultaneous stereological and functional assessments, we demonstrated that both single and especially combined AAS exposure produces multi-level

reproductive toxicity in male mice.

A prominent systemic effect observed in this study was the significant reduction in body weight gain in Test, ND, and especially the Combined groups. In this regard, supraphysiological AAS doses are known to suppress appetite, alter lipid absorption, and promote accelerated fat oxidation. Additionally, strenuous exercise increases energy expenditure and shifts metabolism toward a catabolic state.[33, 34]

Consistent with previous reports,[35, 36] administration of Test, ND, and particularly the triple combination of AAS significantly decreased testicular volume, seminiferous tubule length, and germ cell, Sertoli, and Leydig cell numbers. In this regard, the decline in tubule length and volume reflects shrinkage of the seminiferous epithelium and loss of germ cells. Sertoli cell depletion further compromises micro-environmental support for germ cell survival, while Leydig cell reduction indicates suppressed steroidogenic function and impaired spermatogenesis.[37, 38] These structural changes were accompanied by elevated MDA levels, indicating heightened oxidative stress. Accordingly, oxidative stress–mediated apoptosis, driven by elevated ROS that disrupt mitochondrial function and activate caspase pathways, represents one of the major mechanisms involved.[39] Thus, early spermatogonia remained relatively preserved, consistent with their higher antioxidant capacity,[40] whereas differentiating germ cells and spermatozoa, which possess limited cytoplasmic antioxidants and high polyunsaturated fatty acid content, were more severely affected.[41]

The other key mechanism is suppression of the HPT axis. According to some reports, exogenous AAS suppressed the HPT axis, which reduces intratesticular testosterone essential for spermatogenesis.[5] Strenuous exercise may further exacerbate this suppression by activating the hypothalamic–pituitary–adrenal (HPA) axis and increasing cortisol secretion.[42] These findings are consistent with human studies, where AAS abuse has been shown to suppress gonadotropins and induce a hypogonadal state.[3] Therefore, the combined endocrine disruptions amplify germ-cell depletion and compromise testicular function.

However, serum testosterone measurements in this study revealed complex patterns. While ND showed a slight decrease compared to control, other groups, including Test and Combined AAS, exhibited increased serum levels. These observations suggest that the apparent elevation is likely due to cross-reactivity of ELISA assays with exogenous steroids or their metabolites rather than true endogenous production, as supported by prior evidence that commercial immunoassays cannot fully distinguish between endogenous testosterone and synthetic AAS.[43] Moreover, the concurrent reduction in Leydig cell numbers supports that endogenous steroidogenesis was suppressed rather than enhanced. Importantly, the elevated serum testosterone did not correlate with functional or structural reproductive outcomes, emphasizing that hormonal measurements alone may be misleading when interpreting steroid-induced reproductive toxicity.

Contrary to some previous reports,[44] interstitial tissue volume increased despite the reduction in Leydig cell numbers. This pattern suggests interstitial edema and vascular permeability, most likely secondary to ROS-mediated inflammation. ROS-induced endothelial dysfunction and increased vascular permeability likely contributed to this expansion.[45] The reduction in Leydig cell numbers may be related to oxidative stress and suppressed LH that diminished trophic support,[46, 47] indicating that chronic AAS exposure shifts the interstitial microenvironment toward degenerative rather than proliferative change.

Marked hypertrophy of the prostate and seminal vesicles was evident in all AAS-treated groups, with the Combined regimen producing the largest increases. These structural changes are most likely driven by excessive androgen receptor activation, leading to epithelial proliferation, stromal expansion, and increased secretory activity.[48-50] Similarly, our histological analysis revealed hyperplasia, hypertrophy, and epithelial irregularities in the dorsolateral prostate, while the anterior lobe exhibited luminal dilation, decreased folding, and epithelial thickness, particularly in the ND and Combined AAS groups. The substantial increase in prostatic luminal surface and vascularization further indicates androgen-driven angiogenesis and glandular remodeling.[48, 49]

The structural alterations in these organs were accompanied by significant functional impairments. Sperm count was markedly reduced in Test, ND, and Combined groups, while sperm motility, viability, morphology, and chromatin condensation were impaired across all AAS-treated mice. Consistent with our observations, human studies have also reported reduced sperm concentration and quality following AAS abuse.[3, 4] Excessive ROS impairs sperm function through membrane lipid peroxidation and damage to mitochondrial and tail protein structures.[51] The chromatin condensation defects may reflect protamine deficiency, which increases DNA susceptibility

to fragmentation and compromises its integrity. These deficits translate directly into reduced fertility potential.[27]

Consistent with sperm dysfunction, embryo development was severely compromised. Fertilization rates, cleavage progression, and embryo quality declined substantially in the Test, ND, and especially the Combined group. In agreement with our results, other studies have documented that declines in sperm count, motility, viability, and even normal morphology were associated with diminished fertilization capacity.[1, 52] Arrest at the 2–4-cell stage and reduced 8-cell embryo formation strongly indicate compromised paternal genome activation. It is consistent with evidence showing that sperm oxidative damage, DNA fragmentation, and protamine deficiency interfere with paternal genome activation and early embryonic cell divisions.[53, 54] These findings confirm that AAS-induced sperm defects extend beyond structural abnormalities to functional reproductive failure.

Collectively, these findings demonstrate that the severity of reproductive toxicity is markedly exacerbated by multi-drug AAS stacking under exercise-induced stress. Combined AAS exposure produced the most severe structural and functional impairments, followed by ND and Test alone, with TR exerting comparatively milder effects. These differences may reflect the pharmacokinetics, receptor affinities, and progestogenic activity of each compound.[55] Moreover, exercise intensity and duration modulate the extent of reproductive disruption, underscoring the additive risks of combining strenuous physical activity with AAS misuse.

Despite the valuable insights provided by the present study, several limitations should be acknowledged. First, serum testosterone measurement showed fluctuations and proved to be an unreliable parameter for reflecting HPT axis changes and fertility status. Therefore, complementary markers such as FSH, LH, molecular indicators, and genes related to steroidogenesis are recommended for future studies. Second, the intervention duration was relatively short, preventing evaluation of long-term effects or reversibility of the observed complications.

Conclusion

This study defines AAS–induced male infertility by demonstrating that reproductive toxicity extends to functional failure of fertilization and early embryo development. Through the combined use of unbiased stereological analysis and IVF-based embryo evaluation, we showed that multi-drug AAS stacking under exercise conditions produces synergistic reproductive damage that cannot be inferred from endocrine measurements alone. Importantly, the observed dissociation between circulating androgen levels and reproductive competence highlights a critical limitation of hormone-based fertility assessment in the context of exogenous steroid exposure. Future studies could aim to determine threshold levels at which AAS-induced semen parameter alterations translate into impairments in fertilization and early embryo development, providing clinically relevant guidance for fertility risk assessment in AAS users.

Acknowledgment

The authors sincerely thank the Research Deputy of Shiraz University of Medical Sciences for their support and research grant (Grant number: 25150). This work was carried out by Leila Najafi as part of the requirements for her PhD degree. Special thanks to Mr. Saeed Karbalay-Doust and Dr. Maryam Naseh for their valuable stereological assistance; to Dr. Amini, a veterinary pathologist, for her valuable pathological evaluation; to Ms. Fatemeh Hosseini for her expert supervision of the statistical analyses; and to Ms. Mahboobeh Gholamhosseini and Ms. Hamideh Homayoun for technical support.

Authors' Contribution

L.N. performed the experiments, conducted the statistical analyses, and drafted the initial manuscript. T.E. conceptualized and designed the study and supervised its overall execution. F.D., as the corresponding author, supervised the stereological evaluations and contributed to the manuscript revision and editing. S.B. supervised the sperm analysis and reproductive evaluations, and contributed to data interpretation. N.K. contributed by training and overseeing the assays related to MDA measurement. All authors have reviewed the final version. All authors have read and approved the final manuscript and agree to be accountable for all aspects of the work in ensuring that questions related to the accuracy or integrity of any part of the work are appropriately investigated and resolved.

Declaration of AI

We used ChatGPT (GPT-4) solely for language polishing and grammar checking to improve the clarity and readability. No AI was used for data analysis, interpretation, or content generation.

Conflict of Interest: None declared.

References

1 Agarwal A, Baskaran S, Parekh N, Cho CL, Henkel R, Vij S, et al. Male infertility. Lancet. 2021;397:319-33. doi: 10.1016/S0140-6736(20)32667-2. PubMed PMID: 33308486.

2 Abedpoor N, Taghian F, Hajibabaie F. Exploring the dynamics of exercise intensity on male fertility and reproductive health: advancements and implications for fertility research. Front Reprod Health. 2024;6:1423916. doi: 10.3389/frph.2024.1423916. PubMed PMID: 39091284; PubMed Central PMCID: PMC11291361.

3 Sansone A, Sansone M, Vaamonde D, Sgro P, Salzano C, Romanelli F, et al. Sport, doping and male fertility. Reprod Biol Endocrinol. 2018;16:114. doi: 10.1186/s12958-018-0435-x. PubMed PMID: 30415644; PubMed Central PMCID: PMC6231265.

4 El Osta R, Almont T, Diligent C, Hubert N, Eschwege P, Hubert J. Anabolic steroids abuse and male infertility. Basic Clin Androl. 2016;26:2. doi: 10.1186/s12610-016-0029-4. PubMed PMID: 26855782; PubMed Central PMCID: PMC4744441.

5 Christou MA, Christou PA, Markozannes G, Tsatsoulis A, Mastorakos G, Tigas S. Effects of Anabolic Androgenic Steroids on the Reproductive System of Athletes and Recreational Users: A Systematic Review and Meta-Analysis. Sports Med. 2017;47:1869-83. doi: 10.1007/s40279-017-0709-z. PubMed PMID: 28258581.

6 Ludwig DJ. The effect of androgen on spermatogenesis. Endocrinology. 1950;46:453-81. doi: 10.1210/endo-46-5-453. PubMed PMID: 15414821.

7 Oda SS, El-Ashmawy IM. Adverse effects of the anabolic steroid, boldenone undecylenate, on reproductive functions of male rabbits. Int J Exp Pathol. 2012;93:172-8. doi: 10.1111/j.1365-2613.2012.00814.x. PubMed PMID: 22583130; PubMed Central PMCID: PMC3385914.

8 Rahnema CD, Crosnoe LE, Kim ED. Designer steroids - over-the-counter supplements and their androgenic component: review of an increasing problem. Andrology. 2015;3:150-5. doi: 10.1111/andr.307. PubMed PMID: 25684733.

9 Sjodin B, Hellsten Westing Y, Apple FS. Biochemical mechanisms for oxygen free radical formation during exercise. Sports Med. 1990;10:236-54. doi: 10.2165/00007256-199010040-00003. PubMed PMID: 2247725.

10 Pey A, Saborido A, Blazquez I, Delgado J, Megias A. Effects of prolonged stanozolol treatment on antioxidant enzyme activities, oxidative stress markers, and heat shock protein HSP72 levels in rat liver. J Steroid Biochem Mol Biol. 2003;87:269-77. doi: 10.1016/j.jsbmb.2003.09.001. PubMed PMID: 14698208.

11 Naraghi MA, Abolhasani F, Kashani I, Anarkooli IJ, Hemadi M, Azami A, et al. The effects of swimming exercise and supraphysiological doses of nandrolone decanoate on the testis in adult male rats: a transmission electron microscope study. Folia Morphol (Warsz). 2010;69:138-46. PubMed PMID: 21154283.3

12 Najafi L, Halvaei I, Movahedin M. Canthaxanthin protects human sperm parameters during cryopreservation. Andrologia. 2019;51:e13389. doi: 10.1111/and.13389. PubMed PMID: 31402476.

13 Yuan S, Zhan J, Zhang J, Liu Z, Hou Z, Zhang C, et al. Human zygotic genome activation is initiated from paternal genome. Cell Discov. 2023;9:13. doi: 10.1038/s41421-022-00494-z. PubMed PMID: 36717546; PubMed Central PMCID: PMC9887001.

14 Aitken RJ, De Iuliis GN. Origins and consequences of DNA damage in male germ cells. Reprod Biomed Online. 2007;14:727-33. doi: 10.1016/s1472-6483(10)60676-1. PubMed PMID: 17579989.

15 Alves FL, Oliveira MAF, de Morais ANP, Martins SD, de Sa NAR, Ceccatto VM, et al. Supraphysiological doses of nandrolone decanoate disrupts spermatogenesis but did not interfere on embryo rate. Naunyn Schmiedebergs Arch Pharmacol. 2024;397:4025-34. doi: 10.1007/s00210-023-02847-1. PubMed PMID: 37999756.

16 Rahim SA. Physiological and histological toxic effects of different doses of nandrolone decanoate on the kidney of male mice. Syst Rev Pharm. 2020;11:1927-31.

17 Ismail MA, Al-Khuzaie JHR. Effect of different concentrations of nandrolone decanoate on weights the testes and epididymis of male white mice infected with the protoscolices of the Echinococcus granulosus. J Pharm Sci Res. 2018;10:3277-80.

18 Borodi G, Turza A, Camarasan PA, Ulici A. Structural studies of trenbolone, trenbolone acetate, hexahydrobenzylcarbonate and enanthate esters. J Mol Struct. 2020;1212:128127. doi: 10.1016/j.molstruc.2020.128127.

19 Nair AB, Jacob S. A simple practice guide for dose conversion between animals and human. J Basic Clin Pharm. 2016;7:27-31. doi: 10.4103/0976-0105.177703. PubMed PMID: 27057123; PubMed Central PMCID: PMC4804402.
20 Ogunsuyi OM, Ogunsuyi OI, Akanni O, Alabi OA, Alimba CG, Adaramoye OA, et al. Alteration of sperm parameters and reproductive hormones in Swiss mice via oxidative stress after co-exposure to titanium dioxide and zinc oxide nanoparticles. Andrologia. 2020;52:e13758. doi: 10.1111/and.13758. PubMed PMID: 32671885.
21 Hess RA, Chen P. Computer tracking of germ cells in the cycle of the seminiferous epithelium and prediction of changes in cycle duration in animals commonly used in reproductive biology and toxicology. J Androl. 1992;13:185-90. doi: 10.1002/j.1939-4640.1992.tb00297.x. PubMed PMID: 1601739.
22 Damiao B, Rossi-Junior WC, Guerra FDR, Marques PP, Nogueira DA, Esteves A. Anabolic steroids and their effects of on neuronal density in cortical areas and hippocampus of mice. Braz J Biol. 2021;81:537-43. doi: 10.1590/1519-6984.224642. PubMed PMID: 32876164.
23 Onaolapo OJ, Onaolapo AY, Omololu TA, Oludimu AT, Segun-Busari T, Omoleke T. Exogenous Testosterone, Aging, and Changes in Behavioral Response of Gonadally Intact Male Mice. J Exp Neurosci. 2016;10:59-70. doi: 10.4137/JEN.S39042. PubMed PMID: 27158222; PubMed Central PMCID: PMC4854217.
24 Malmir M, Faraji T, Noreini N, Mehranjani S. Protective antioxidant effects of N-acetylcysteine on testicular tissue and serum testosterone in paranonylphenol-treated mice (a stereological analysis). Reprod Syst Sex Disord. 2018;7:1000225.
25 Rahimipour M, Talebi AR, Anvari M, Sarcheshmeh AA, Omidi M. Effects of different doses of ethanol on sperm parameters, chromatin structure and apoptosis in adult mice. Eur J Obstet Gynecol Reprod Biol. 2013;170:423-8. doi: 10.1016/j.ejogrb.2013.06.038. PubMed PMID: 23871382.
26 Mehraban Z, Ghaffari Novin M, Golmohammadi MG, Sagha M, Pouriran K, Nazarian H. Protective effect of gallic acid on apoptosis of sperm and in vitro fertilization in adult male mice treated with cyclophosphamide. J Cell Biochem. 2019;120:17250-7. doi: 10.1002/jcb.28987. PubMed PMID: 31135067.
27 Kooshesh L, Bahmanpour S, Zeighami S, Nasr-Esfahani MH. Effect of Letrozole on sperm parameters, chromatin status and ROS level in idiopathic Oligo/Astheno/Teratozoospermia. Reprod Biol Endocrinol. 2020;18:47. doi: 10.1186/s12958-020-00591-2. PubMed PMID: 32404173; PubMed Central PMCID: PMC7218838.
28 Sargazi M, Karbalaei N, Karbalay-Doust S, Keshtgar S, Aghaei Z. Wharton's Jelly Mesenchymal Stem Cell Conditioned Medium Ameliorates Diabetes-Induced Testicular Damage and Sperm Abnormalities by Mitigating Oxidative Stress, Apoptosis, and Inflammation. Stem Cells Int. 2024;2024:7084913. doi: 10.1155/2024/7084913. PubMed PMID: 39391856; PubMed Central PMCID: PMC11466552.
29 Dehghani F, Hassanpour A, Poost-Pasand A, Noorafshan A, Karbalay-Doust S. Protective effects of L-carnitine and homogenized testis tissue on the testis and sperm parameters of busulfan-induced infertile male rats. Iran J Reprod Med. 2013;11:693-704. PubMed PMID: 24639808; PubMed Central PMCID: PMC3941323.
30 Karbalay-Doust S, Noorafshan A. Stereological study of the effects of nandrolone decanoate on the rat prostate. Micron. 2006;37:617-23. doi: 10.1016/j.micron.2006.02.005. PubMed PMID: 16597504.
31 Nasiri N, Eftekhari-Yazdi P. An overview of the available methods for morphological scoring of pre-implantation embryos in in vitro fertilization. Cell J. 2015;16:392-405. doi: 10.22074/cellj.2015.486. PubMed PMID: 25685730; PubMed Central PMCID: PMC4297478.
32 Desai NN, Goldstein J, Rowland DY, Goldfarb JM. Morphological evaluation of human embryos and derivation of an embryo quality scoring system specific for day 3 embryos: a preliminary study. Hum Reprod. 2000;15:2190-6. doi: 10.1093/humrep/15.10.2190. PubMed PMID: 11006197.
33 Magalhaes SC, de Oliveira KA, Freiras PA, Moreira Gomes MD, Pereira LM, Boa LF, et al. High-dose Nandrolone Decanoate induces oxidative stress and inflammation in retroperitoneal adipose tissue of male rats. J Steroid Biochem Mol Biol. 2020;203:105728. doi: 10.1016/j.jsbmb.2020.105728. PubMed PMID: 32712213.
34 Pozzi R, Fernandes L, Cavalcante da Silva V, D'Almeida V. Nandrolone decanoate and resistance exercise affect body composition and energy metabolism. Steroids. 2021;174:108899. doi: 10.1016/j.

steroids.2021.108899. PubMed PMID: 34358557.
35 Noorafshan A, Karbalay-Doust S, Ardekani FM. High doses of nandrolone decanoate reduce volume of testis and length of seminiferous tubules in rats. APMIS. 2005;113:122-5. doi: 10.1111/j.1600-0463.2005.apm1130205.x. PubMed PMID: 15723686.
36 Shokri S, Mokhtari T, Azizi M, Abbaszadeh H-a, Moayeri A. Nandrolone decanoate administration can increase apoptosis in spermatogenesis cell lines in male rats. J Basic Res Med Sci. 2014;1:21-31.
37 O'Donnell L, Smith LB, Rebourcet D. Sertoli cells as key drivers of testis function. Semin Cell Dev Biol. 2022;121:2-9. doi: 10.1016/j.semcdb.2021.06.016. PubMed PMID: 34229950.
38 Walker WH. Testosterone signaling and the regulation of spermatogenesis. Spermatogenesis. 2011;1:116-20. doi: 10.4161/spmg.1.2.16956. PubMed PMID: 22319659; PubMed Central PMCID: PMC3271653.
39 Shaha C, Tripathi R, Mishra DP. Male germ cell apoptosis: regulation and biology. Philos Trans R Soc Lond B Biol Sci. 2010;365:1501-15. doi: 10.1098/rstb.2009.0124. PubMed PMID: 20403866; PubMed Central PMCID: PMC2871916.
40 Celino FT, Yamaguchi S, Miura C, Ohta T, Tozawa Y, Iwai T, et al. Tolerance of spermatogonia to oxidative stress is due to high levels of Zn and Cu/Zn superoxide dismutase. PLoS One. 2011;6:e16938. doi: 10.1371/journal.pone.0016938. PubMed PMID: 21364994; PubMed Central PMCID: PMC3041797.
41 Wang Y, Fu X, Li H. Mechanisms of oxidative stress-induced sperm dysfunction. Front Endocrinol (Lausanne). 2025;16:1520835. doi: 10.3389/fendo.2025.1520835. PubMed PMID: 39974821; PubMed Central PMCID: PMC11835670.
42 Hackney AC. Hypogonadism in Exercising Males: Dysfunction or Adaptive-Regulatory Adjustment? Front Endocrinol (Lausanne). 2020;11:11. doi: 10.3389/fendo.2020.00011. PubMed PMID: 32082255; PubMed Central PMCID: PMC7005256.
43 Krasowski MD, Drees D, Morris CS, Maakestad J, Blau JL, Ekins S. Cross-reactivity of steroid hormone immunoassays: clinical significance and two-dimensional molecular similarity prediction. BMC Clin Pathol. 2014;14:33. doi: 10.1186/1472-6890-14-33. PubMed PMID: 25071417; PubMed Central PMCID: PMC4112981.
44 Mohamed HM, Mohamed MA. Effect of different doses of nandrolone decanoate on lipid peroxidation, DNA fragmentation, sperm abnormality and histopathology of testes of male Wister rats. Exp Toxicol Pathol. 2015;67:1-11. doi: 10.1016/j.etp.2014.09.003. PubMed PMID: 25440442.
45 El-Shahat AE-R, Gabr A, Meki A-R, Mehana E-S. Altered testicular morphology and oxidative stress induced by cadmium in experimental rats and protective effect of simultaneous green tea extract. Int J Morphol. 2009;27:757. doi: 10.4067/S0717-95022009000300020.
46 Tapanainen JS, Tilly JL, Vihko KK, Hsueh AJ. Hormonal control of apoptotic cell death in the testis: gonadotropins and androgens as testicular cell survival factors. Mol Endocrinol. 1993;7:643-50. doi: 10.1210/mend.7.5.8316250. PubMed PMID: 8316250.
47 Janjic MM, Stojkov NJ, Andric SA, Kostic TS. Anabolic-androgenic steroids induce apoptosis and NOS2 (nitric-oxide synthase 2) in adult rat Leydig cells following in vivo exposure. Reprod Toxicol. 2012;34:686-93. doi: 10.1016/j.reprotox.2012.10.003. PubMed PMID: 23085480.
48 Franck-Lissbrant I, Haggstrom S, Damber JE, Bergh A. Testosterone stimulates angiogenesis and vascular regrowth in the ventral prostate in castrated adult rats. Endocrinology. 1998;139:451-6. doi: 10.1210/endo.139.2.5683. PubMed PMID: 9449610.
49 Justulin LA, Jr., Ureshino RP, Zanoni M, Felisbino SL. Differential proliferative response of the ventral prostate and seminal vesicle to testosterone replacement. Cell Biol Int. 2006;30:354-64. doi: 10.1016/j.cellbi.2006.01.002. PubMed PMID: 16546411.
50 Neubauer B, Mawhinney M. Actions of androgen and estrogen on guinea pig seminal vesicle epithelium and muscle. Endocrinology. 1981;108:680-7. doi: 10.1210/endo-108-2-680. PubMed PMID: 6161002.
51 Walke G, Gaurkar SS, Prasad R, Lohakare T, Wanjari M. The Impact of Oxidative Stress on Male Reproductive Function: Exploring the Role of Antioxidant Supplementation. Cureus. 2023;15:e42583. doi: 10.7759/cureus.42583. PubMed PMID: 37641770; PubMed Central PMCID: PMC10460465.
52 Parinaud J, Mieusset R, Vieitez G, Labal B, Richoilley G. Influence of sperm parameters on embryo quality. Fertil Steril. 1993;60:888-92. doi: 10.1016/s0015-0282(16)56292-x. PubMed PMID: 8224276.
53 Lismer A, Kimmins S. Emerging evidence that the mammalian sperm epigenome

serves as a template for embryo development. Nat Commun. 2023;14:2142. doi: 10.1038/s41467-023-37820-2. PubMed PMID: 37059740; PubMed Central PMCID: PMC10104880.
54 Colaco S, Sakkas D. Paternal factors contributing to embryo quality. J Assist Reprod Genet. 2018;35:1953-68. doi: 10.1007/s10815-018-1304-4. PubMed PMID: 30206748; PubMed Central PMCID: PMC6240539.
55 Kicman AT. Pharmacology of anabolic steroids. Br J Pharmacol. 2008;154:502-21. doi: 10.1038/bjp.2008.165. PubMed PMID: 18500378; PubMed Central PMCID: PMC2439524.